ISAS - INTERNATIONAL SCHOOL
FOR ADVANCED STUDIES

Density Functional Theory without orbitals: a path towards very large scale electronic structure calculations

Thesis submitted for the degree of

"Magister Philosophiæ"

CANDIDATE

Alberto Franceschetti

SUPERVISOR

Prof. Stefano Baroni

April 1992

TRIESTE

SISSA - SCUOLA
INTERNAZIONALE
SUPERIORE
STUDI AVANZATI
TRIESTE
Strada Costiera 11

SISSA ISAS
SCUOLA INTERNAZIONALE SUPERIORE DI STUDI AVANZATI
INTERNATIONAL SCHOOL FOR ADVANCED STUDIES

Density Functional Theory without orbitals: a path towards very large scale electronic structure calculations

Thesis submitted for the degree of

"Magister Philosophiæ"

CANDIDATE

Alberto Franceschetti

SUPERVISOR

Prof. Stefano Baroni

April 1992

Introduction

In the last few years there has been an increasing interest in the possibility of performing self-consistent calculations in the density-functional scheme without invoking orbitals [1-7]. The conventional approach to the first-principles calculation of ground state properties relies on the solution of the one-electron Kohn-Sham equation

$$\left[-\frac{1}{2}\nabla^2 + v_{eff}(\mathbf{x})\right] \psi_\alpha(\mathbf{x}) = \varepsilon_\alpha \psi_\alpha(\mathbf{x}) \,, \tag{1}$$

where

$$v_{eff}(\mathbf{x}) = v_{ext}(\mathbf{x}) + \int \frac{n(\mathbf{x}')}{|\mathbf{x}-\mathbf{x}'|}\, d\mathbf{x}' + v_{xc}(n(\mathbf{x})) \,. \tag{2}$$

The charge density is then recovered from the single-particle wavefunctions $\psi_\alpha(\mathbf{x})$ by the ansatz

$$n(\mathbf{x}) = \sum\nolimits_\alpha |\psi_\alpha(\mathbf{x})|^2 \; \theta(\varepsilon_F - \varepsilon_\alpha) \,, \tag{3}$$

ε_F being the Fermi energy, and a new iteration is started with the effective potential obtained from eq. (2).

From a computational point of view, the time consuming part of this strategy is the solution of the Kohn-Sham equation, which is generally accomplished by expanding the single-particle wavefunctions $\psi_\alpha(\mathbf{x})$ in some appropriate basis set and calculating the eigenvalues and eigenvectors of the hamiltonian matrix in this representation. With the use of iterative diagonalization techniques, the workload needed for the evaluation of the occupied single-particle wavefunctions is proportional to NM^2, where N is the dimension of the basis set and M is the number of occupied states; this is due to the fact that the orbitals have to be kept orthogonal during iteration. Since both N and M are proportional to

the number of atoms in the unit cell (N_{at}), the computational effort required by the orbital approach to the Kohn-Sham equation scales as N_{at}^3.

In principle, within density-functional theory, the ground state properties of an interacting electron system are completely determined by the charge density, which plays the role of a basic variable. Therefore it should be possible to bypass the Kohn-Sham orbitals, and to devise an algorithm leading directly to the charge density. Since the local density of states at a given point, as pointed out by Friedel [8], is a stable quantity with respect to a variation of the boundary conditions far from that point, this algorithm would naturally scale linearly with the size of the system.

Let $G(\mathbf{x},\mathbf{x}';z)$ be the real-space representation of the Green's function associated with the Kohn-Sham hamiltonian $H_{eff} = -\frac{1}{2}\nabla^2 + v_{eff}(\mathbf{x})$:

$$G(\mathbf{x},\mathbf{x}';z) \equiv \langle \mathbf{x}|G(z)|\mathbf{x}'\rangle = \langle \mathbf{x}|\left(z - H_{eff}\right)^{-1}|\mathbf{x}'\rangle \ . \tag{4}$$

In terms of the Kohn-Sham eigenvalues ε_α and eigenfunctions $\psi_\alpha(\mathbf{x})$, the Green's function reads:

$$G(\mathbf{x},\mathbf{x}';z) = \sum\nolimits_\alpha \frac{\psi_\alpha(\mathbf{x})\,\psi_\alpha^\star(\mathbf{x}')}{z-\varepsilon_\alpha} \ . \tag{5}$$

The charge density $n(\mathbf{x})$ has a simple expression in terms of the diagonal elements of the Green's function:

$$n(\mathbf{x}) = 2\,\frac{1}{2\pi i}\int_{\mathcal{C}} G(\mathbf{x},\mathbf{x};z)\,dz \ , \tag{6}$$

where the factor 2 accounts for spin degeneracy, and $\mathcal{C}$ is an integration contour in the complex energy plane enclosing the whole spectrum up to the Fermi energy. Eq. (6) is readily proved starting from eq. (5) and making use of the theorem of residues.

In order to get an algorithm which scales linearly with the size of the system, the workload required for the evaluation of the integral appearing in eq. (6) must not depend on the size of the system. The number of points at which $G(\mathbf{x},\mathbf{x};z)$ has to be sampled depends on:

i) the length of the integration contour $\mathcal{C}$, which is related to the width of the valence band;

ii) the smoothness of the Green's function along the integration contour $\mathcal{C}$.

Actually, the valence band width is an intensive quantity which does not depend on the volume of the system. On the other hand, $G(\mathbf{x},\mathbf{x};z)$ is a smooth function of z, provided the integration path is kept well apart from the energy spectrum [9,10]. Therefore, we can conclude that, at least for insulators, the evaluation of the integral is independent of the size of the system.

An efficient way of computing the Green's function $G(\mathbf{x},\mathbf{x};z)$ with a workload which is independent of the size of the system is provided by the recursion method [11-13]. The next chapter will be devoted to a brief description of this method.

The recursion method

The recursion method (RM) provides a simple and powerful technique for calculating the expectation value of the Green's operator $G(z)$ on a generic state $|0\rangle$. Given the hamiltonian H and the starting state $|0\rangle$, both expressed in some appropriate basis set $\{|\varphi_k\rangle,\ k = 1,\ldots,N\}$, the recursion method generates a chain of states $|0\rangle, |1\rangle, |2\rangle, \ldots, |n\rangle, \ldots$ by the three-term recurrence relation

$$H|n\rangle = a_n|n\rangle + b_{n+1}|n+1\rangle + b_n|n-1\rangle \ . \tag{7}$$

It is easy to show that the coefficients $\{a_n, b_n\}$ can be chosen so as to guarantee the orthonormality of the states of the chain;to this end, it is enough to put

$$\begin{aligned} a_n &= \langle n|H|n\rangle \\ b_{n+1} &= \| \ (H - a_n)\,|n\rangle \ - b_n\,|n-1\rangle \ \| \ , \end{aligned} \tag{8}$$

where $b_0 = 0$ and $\| \ |u\rangle \ \|$ stands for the norm of the state $|u\rangle$. Carrying on the chain up to the $N-1$ step yields a new orthonormal basis set $\{|n\rangle,\ n = 0,\ldots,N-1\}$ which spans the same Hilbert space as the original basis set (Lanczos method). In the representation of the chain states, the hamiltonian H turns out to be tridiagonal, with

$$\begin{aligned} H_{n,n} &= a_n \\ H_{n,n+1} &= H_{n+1,n} = b_{n+1} \ . \end{aligned} \tag{9}$$

Using the properties of tridiagonal matrices it is easy to show that Green's function matrix projected upon the first n states of the chain is given by

$$G^{(n)}(z) = \begin{pmatrix} z-a_0 & -b_1 & \ldots & 0 & 0 \\ -b_1 & z-a_1 & \ldots & 0 & 0 \\ \vdots & \vdots & \ddots & \vdots & \vdots \\ 0 & 0 & \ldots & z-a_{n-1} & -b_n \\ 0 & 0 & \ldots & -b_n & z-a_n-t_n(z) \end{pmatrix}^{-1} , \tag{10}$$

where $t_n(z)$, the so called *terminator*, accounts for the remaining part of the chain:

$$t_n(z) = \cfrac{b_{n+1}^2}{z - a_{n+1} - \cfrac{b_{n+2}^2}{z - a_{n+2} - \cdots}} \,. \tag{11}$$

In particular, the diagonal element of the Green's function $G_{0,0}(z) \equiv \langle 0|G(z)|0\rangle$ is given by the continued fraction

$$G_{0,0}(z) = \cfrac{1}{z - a_0 - \cfrac{b_1^2}{z - a_1 - \cfrac{b_2^2}{z - a_2 - \cdots - t_n(z)}}} \,. \tag{12}$$

Since the far states of the chain contribute lower and lower to the local density of states projected upon the starting state, the continued fraction (12) turns out to be rapidly converging, at least for energy values quite apart from the spectrum.

Now suppose that, having obtained the first n states of the chain, one aims to evaluate the terminator $t_n(z)$ using a different set of orthonormal basis vectors $\{|\tilde{\varphi}_k\rangle\}$. The most obvious way to do this is to project the last two states of the chain on the space spanned by the vectors $\{|\tilde{\varphi}_k\rangle\}$:

$$\begin{aligned} |n-1\rangle \to |\tilde{0}\rangle &= \sum\nolimits_k |\tilde{\varphi}_k\rangle\langle\tilde{\varphi}_k|n-1\rangle \\ |n\rangle \to |\tilde{1}\rangle &= \sum\nolimits_k |\tilde{\varphi}_k\rangle\langle\tilde{\varphi}_k|n\rangle \,, \end{aligned} \tag{13}$$

and to generate a new chain starting from the states $|\tilde{0}\rangle, |\tilde{1}\rangle$ and using the projected hamiltonian $\tilde{H}$. The terminator is then given by

$$t_n(z) = \tilde{t}_1(z) \,. \tag{14}$$

Care must be taken when the space spanned by the vectors $\{|\tilde{\varphi}_k\rangle\}$ is different from the previous one. In this case the states $|\tilde{0}\rangle$ and $|\tilde{1}\rangle$, as defined by eq.

(13), are no more orthogonal to each other and to the preceding states of the chain, so that the definition of the states $|\tilde{0}\rangle$, $|\tilde{1}\rangle$ and of the hamiltonian $\tilde{H}$ is to some extent arbitrary.

An alternative approach to the evaluation of the terminator consists in calculating the Green's function diagonal element $G_{n,n}(z) \equiv \langle n|G(z)|n\rangle$ by starting a new chain from the state $|\tilde{0}\rangle = \sum_k |\tilde{\varphi}_k\rangle\langle\tilde{\varphi}_k|n\rangle$ with the projected hamiltonian $\tilde{H}$. The terminator is then recovered from the expression

$$t_n(z) = \frac{G_{n,n}(z) - c_n(z)}{G_{n,n}(z)\, c_n(z)} , \tag{15}$$

where $c_n(z)$ is the *inverse chain*

$$c_n(z) = \cfrac{1}{z - a_n - \cfrac{b_n^2}{z - a_{n-1} - \cfrac{b_{n-1}^2}{z - a_{n-2} - \cdots}}} . \tag{16}$$

It is also possible to write down $t_n(z)$ in terms of $G_{n+1,n+1}(z)$ [7]:

$$t_n(z) = \frac{b_{n+1}^2\, G_{n+1,n+1}(z)}{1 + b_{n+1}^2\, c_n(z)\, G_{n+1,n+1}(z)} . \tag{17}$$

The same problems discussed previously arise when the basis set $\{|\tilde{\varphi}_k\rangle\}$ is not complete with respect to $\{|\varphi_k\rangle\}$.

Calculation of the charge density

In order to evaluate the charge density, the Kohn-Sham hamiltonian has been discretized on a set of points $\{\mathbf{x}_i,\, i = 1,\ldots,N\}$, arranged in a cubic uniform mesh with lattice spacing h. In other words, the basis vectors $\{|\varphi_i\rangle\}$ are simply delta-like functions centered at the grid points $\mathbf{x}_i$:

$$\langle \mathbf{x}|\varphi_i\rangle = \delta(\mathbf{x}-\mathbf{x}_i)\,. \tag{18}$$

These states are obviously orthonormal.

Using a nearest-neighbour discretization of the kinetic energy and a local pseudopotential, the hamiltonian takes up a tight binding form:

$$H = \sum_{i=1}^{N} \varepsilon_i\, |\varphi_i\rangle\langle\varphi_i| + \sum_{i,j=1}^{N} t_{i,j}\, |\varphi_i\rangle\langle\varphi_j|\,, \tag{19}$$

where

$$\begin{aligned} \varepsilon_i &= \frac{3}{h^2} + v_{eff}(\mathbf{x}_i) \\ t_{i,j} &= \begin{cases} -\frac{1}{2h^2} & \text{if } i \text{ and } j \text{ are nearest-neighbours} \\ 0 & \text{otherwise} \end{cases} \end{aligned} \tag{20}$$

The hamiltonian matrix is clearly sparse in this representation. The lattice spacing h has to be chosen in order to give a correct sampling of the charge density without increasing too much the number of mesh points.

For each point $\mathbf{x}_i$ of the real-space mesh, we calculate the Green's function $G(\mathbf{x}_i,\mathbf{x}_i;z)$ employing the recursion method. The starting state of the chain coincides with the localized, delta-like state $|\varphi_i\rangle$. Since the hamiltonian admits only nearest-neighbour hopping, the n-th state of the chain will be localized into a regular octahedron whose diagonal is given by $2hn$, provided the boundaries of the system have not been reached. It is this property, together with the

fact that only a few steps of the recursion chain are needed, that makes this algorithm independent of the size of the system.

The charge density at the point $\mathbf{x}_i$ is then recovered from eq. (6). The integration contour is somewhat arbitrary; our choice is shown in Fig. 1.

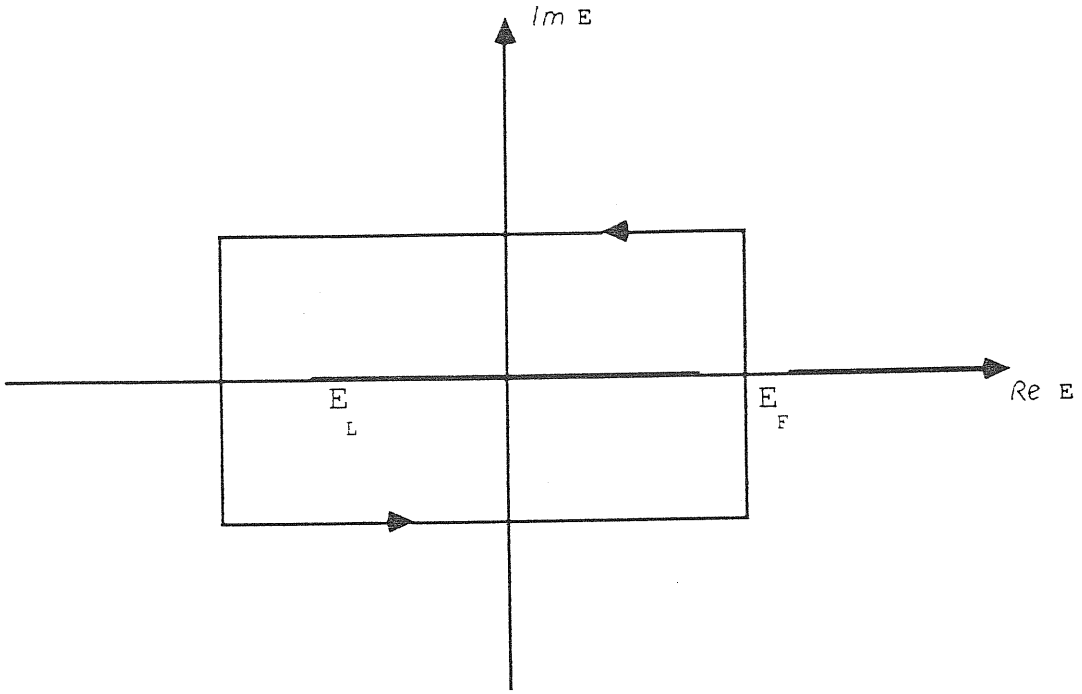

Fig. 1 – *Integration path in the complex energy plane.* E_L *: lower band edge;* E_F *: Fermi energy.*

The integration contour depends basically on the lower band edge E_L, which can be easily estimated, and on the Fermi energy E_F, which has to be calculated from the relation

$$\int n(\mathbf{x})\, d\mathbf{x} = N_{el} \,, \tag{21}$$

N_{el} being the total number of valence electrons.

Results

As a test model, we have chosen a system consisting of 64 Silicon atoms arranged in a cubic cell with lattice parameter $a = 2a_0$, a_0 being the equilibrium lattice parameter of crystalline Si. The atoms are slightly displaced at random from their equilibrium positions to simulate some disorder.

The local ionic pseudopotentials proposed by Appelbaum and Hamann [14] have been used. The effective potential $v_{eff}(\mathbf{x})$ is obtained simply by screening the bare pseudopotential with the Thomas-Fermi diagonal dielectric function. The hamiltonian H has been discretized on a cubic uniform mesh consisting of $32 \times 32 \times 32$ points, with periodic boundary conditions. For comparison, we have calculated the "exact" charge density by a conventional orbital approach, assuming the same form for the hamiltonian matrix. For the computation of the diagonal elements of the Green's function with the recursion method, different choices of the terminator have been tested, as discussed in detail in the following paragraphs. Finally, the contour integral appearing in eq. (6) has been evaluated using an adaptive Simpson's rule, with the value of the Fermi energy chosen in the middle of the energy gap resulting from the orbital calculation.

(a) *Truncation of the continued fraction.*

As a first approach to the calculation of the diagonal Green's function $G(\mathbf{x}_i, \mathbf{x}_i; z)$, we simply truncated the continued fraction after n steps, assuming a vanishing terminator: $t_n(z) = 0$. Only the first n states of the recursion chain are needed. The charge density along the (111) direction is plotted in Fig. 2 for $n = 20$, $n = 80$ and $n = 200$. The values of $n(\mathbf{x})$ were computed for each of the 32 points laying on the diagonal of the cubic cell, and then interpolated using a cubic spline.

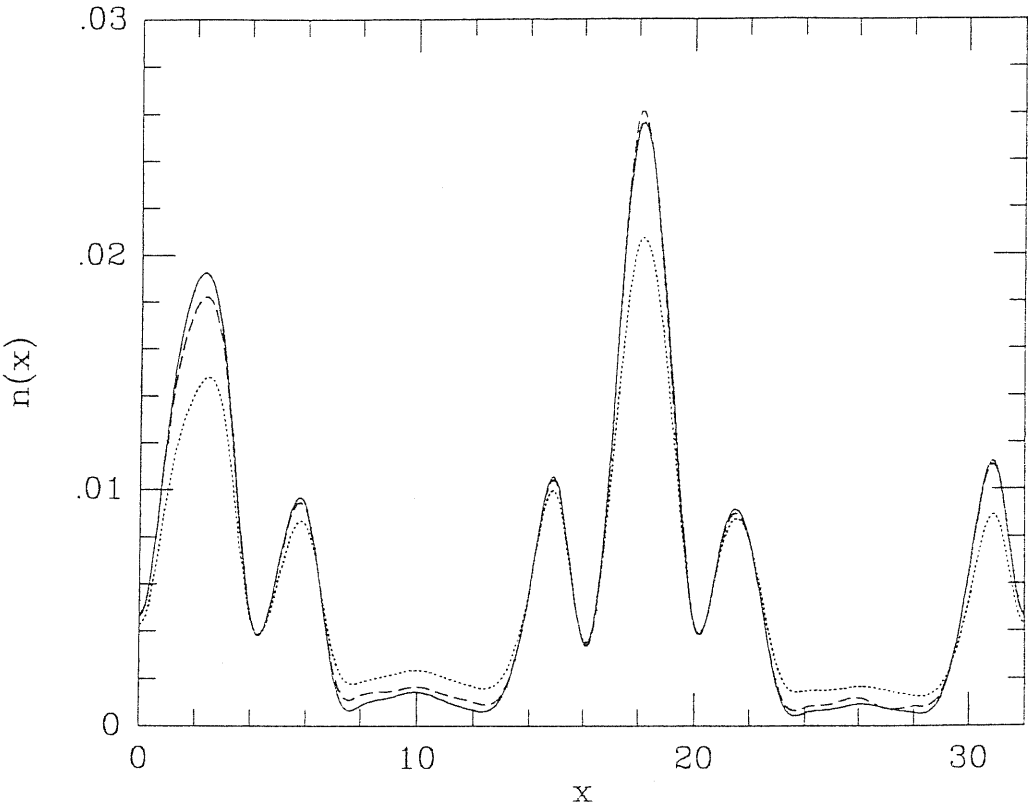

Fig. 2 – *Charge density along the (111) direction obtained from the 20-steps chain (dotted line), 80-steps chain (dashed line) and 200-steps chain (solid line) with vanishing terminators.*

The result for $n = 200$ is practically indistinguishable from the "exact" one, obtained from the orbital calculation.

Though the charge density converges in a well-behaved way to the exact value, this approach shows some unpleasant features. First of all, it is rather demanding from a computational point of view, although each grid point can be treated independently, so that the algorithm is particularly well suited for parallel computation. Since the required workload grows as n^3, at least for

the first steps of the chain, which are not affected by the boundary conditions, it would be extremely important to keep the number of recursion steps as low as possible. Second, and related, the regions far from the starting point are treated with the same accuracy as near regions, though the latter are expected to contribute much more to the charge density at the given point. Finally, no use is made of the fact that the chains starting from neighbouring points contain nearly the same amount of physical information.

(b) *Direct calculation of the terminator.*

As an alternative approach to the calculation of the diagonal Green's function $G(\mathrm{x}_i, \mathrm{x}_i; z)$, we explored the possibility of stopping the recursion chain after a small number of steps and calculating the terminator using a coarser grid. By doubling the lattice spacing, we get a set of orthonormal basis vectors $\{|\tilde{\varphi}_k\rangle,\ k = 1, \ldots, N/8\}$ localized at the nodes of a uniform grid with lattice spacing $2h$. Since the new basis set is not complete with respect to the previous one, the way of rescaling the chain states and the hamiltonian is not obvious; different scaling techniques have been tested, as discussed below.

The charge densities along the (111) direction shown in Fig. 3 and Fig. 4 (dashed lines) have been obtained by truncating the recursion chain after the first 20 steps and calculating the terminator $t_{20}(z)$ on the coarse grid, using two different approximations.

In the first case, the states $|n-1\rangle$ and $|n+1\rangle$ of the first chain, projected upon the new basis set, yielded the vectors $|\tilde{0}\rangle$ and $|\tilde{1}\rangle$; normalizing these states and orthogonalizing them by the ansatz

$$\frac{|\tilde{0}\rangle - \langle\tilde{1}|\tilde{0}\rangle}{\sqrt{1 - |\langle\tilde{1}|\tilde{0}\rangle|^2}} \rightarrow |\tilde{0}\rangle \tag{22}$$

we got the starting vectors for the second chain. The new hamiltonian $\tilde{H}$ was obtained from the previous one assuming the same expression for the kinetic

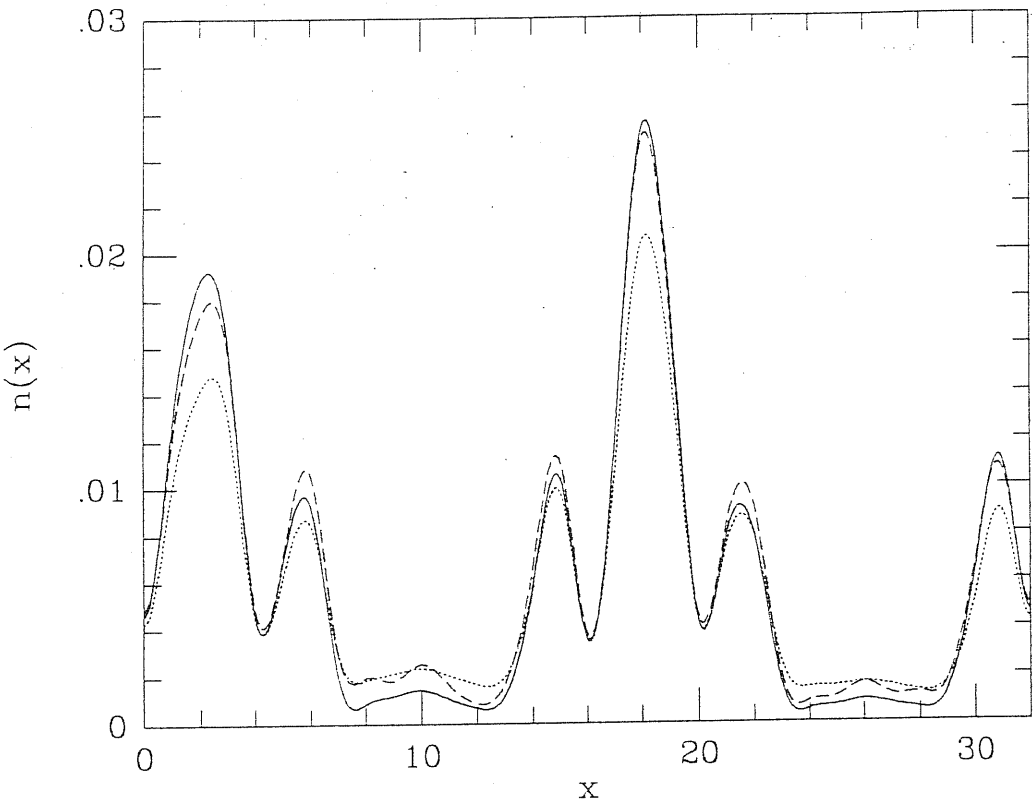

Fig. 3 – *Charge density along the (111) direction obtained from a 20-steps chain with a coarse grid terminator (dashed line). For comparison, the truncated 20-steps chain (dotted line) and 200-steps chain (solid line) results are shown.*

energy, and taking the values of the potential at the coarse grid points. The length of the second chain was determined by a convergence test; 100 steps were proved to be enough to give stable results. Finally, the terminator $t_{20}(z)$ was recovered from the relation $t_{20}(z) = \tilde{t}_0(z)$.

In the second case, the state $|n+1\rangle$ of the first chain was rescaled by averaging its components at the points of the coarse mesh with those at the

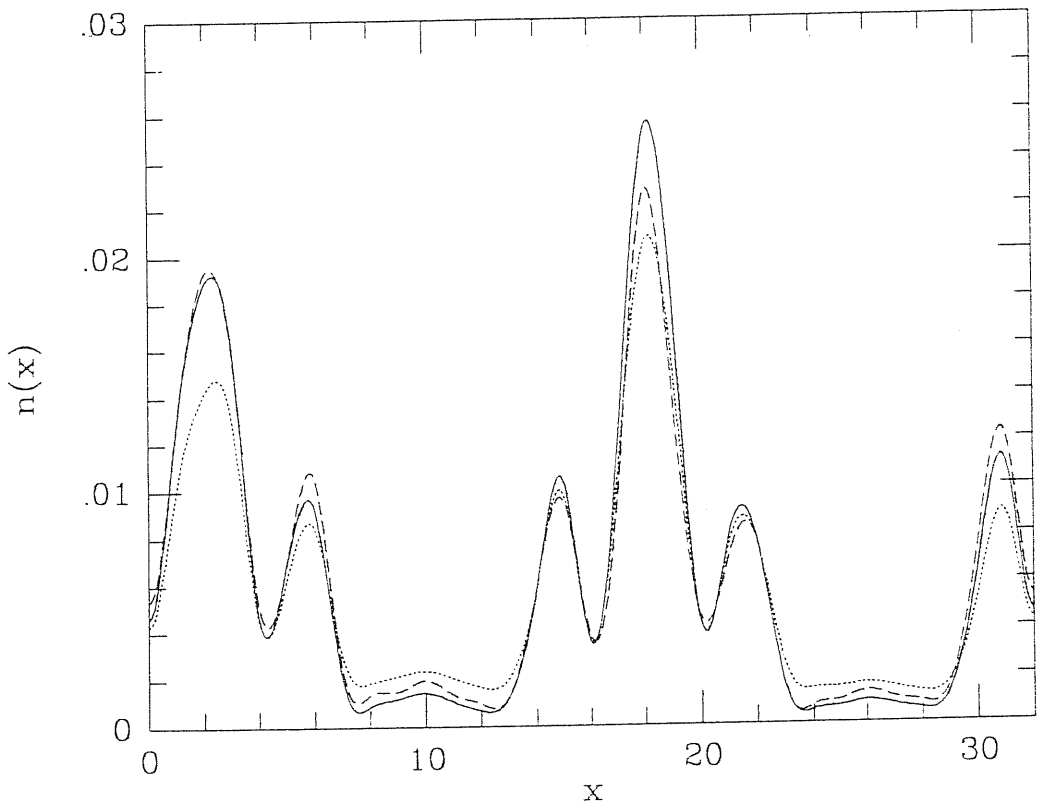

Fig. 4 – *Charge density along the (111) direction obtained from a 20-steps chain with a coarse grid terminator (dashed line). For comparison, the truncated 20-steps chain (dotted line) and 200-steps chain (solid line) results are shown.*

neighbouring points of the fine mesh. The resulting state was normalized to get the starting vector $|\tilde{0}\rangle$ for the second chain. The new hamiltonian $\tilde{H}$ was obtained from the old one assuming the same form of the kinetic energy and averaging the potential as described above. The second chain was truncated after 100 steps, and the terminator $t_{20}(z)$ was obtained from eq. (17).

For comparison, Figs. 3 and 4 show the charge density calculated by trun-

cating the first recursion chain after 20 steps (dotted lines) and 200 steps (solid lines), and assuming a vanishing terminator. The mean square deviation of the charge density with respect to the 200-steps chain result is $\sigma = 0.679 \times 10^{-3}$ in the first case (Fig. 3) and $\sigma = 1.065 \times 10^{-3}$ in the second one (Fig. 4). These values have to be compared with the mean square deviation of the charge density resulting from the 20-steps chain calculation: $\sigma_0 = 1.666 \times 10^{-3}$. Only a little improvement is achieved. There are two possible reasons for this behavior. First, the way of rescaling the chain states and the hamiltonian is probably too rough. Furthermore, the states of the second chain are not orthogonal to those of the first chain, giving a poor description of the region close to the starting point. Possible solutions to these drawbacks are currently under investigation.

(c) *Fitting the terminator.*

The idea of fitting the terminator arises from the observation that $t_n(z)$ is a smooth function of the starting point $\mathbf{x}_i$, provided the complex energy z is chosen far enough from the energy spectrum. Assuming a parametric functional form for the energy dependence of the terminator, one can hopefully fit the parameters in order to reproduce the correct charge density at some given points $\mathbf{x}_i$, $i = 1, \ldots N_s$, with $N_s \ll N$, and assume the same terminator holds for all the remaining points.

In order to test this idea, we have chosen the following quadratic form for the energy dependence of the terminator:

$$t_n(z) = \alpha_n z^2 + \beta_n z + \gamma_n \ , \tag{23}$$

where α_n, β_n and γ_n are complex parameters which have been fitted in order to reproduce the charge density obtained from the 200-steps chain calculation along the (111) direction. The result for $n = 20$ is shown in Fig. 5 (dashed line), together with the charge densities obtained from the 20-steps truncated chain

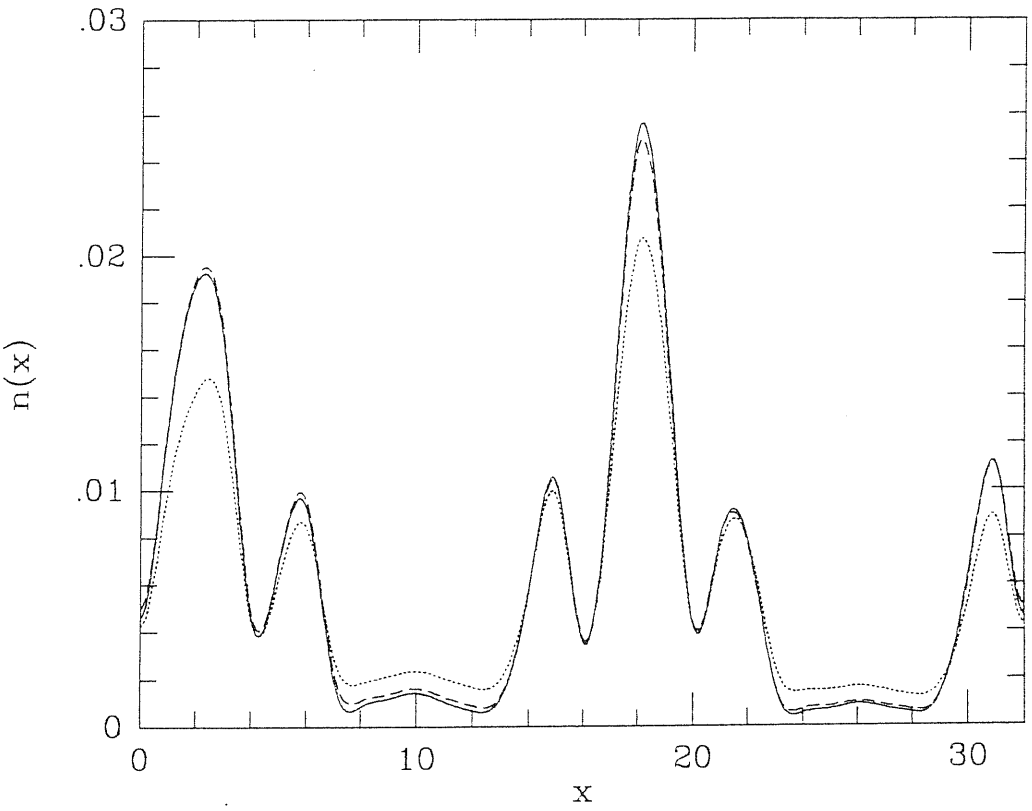

Fig. 5 – *Charge density along the (111) direction obtained from a 20-steps chain with fitted terminator (dashed line). For comparison, the truncated 20-steps chain (dotted line) and 200-steps chain (solid line) results are shown.*

(dotted line) and from the 200-steps truncated chain (solid line). The mean square deviation of the charge density resulting from the 20-steps terminated chain with respect to the 200-steps chain turns out to be $\sigma = 0.266 \times 10^{-3}$, compared with $\sigma_0 = 1.666 \times 10^{-3}$ for the 20-steps truncated chain. A further improvement to this result could be achieved by introducing some dependence of the parametrized terminator upon the position of the starting point.

A self-consistent calculation

As a final test, we have performed a self-consistent calculation on a smaller system, consisting of 8 Silicon atoms arranged in a cubic unit cell with lattice parameter $a_0 = 10.26\,\text{a.u.}$ The atoms are slightly randomly displaced from their equilibrium positions. The hamiltonian has been discretized on a uniform $16 \times 16 \times 16$ mesh, using periodic boundary conditions. The starting potential is obtained from the Appelbaum-Hamann ionic pseudopotentials screened with the Thomas-Fermi dielectric function.

Since the Fermi energy is not known a priori, the following approach to the charge density calculation has been adopted. First of all, a single 24-steps recursion chain for each grid point was carried on. The terminator $t_{24}(z)$ has been fitted using a complex constant: $t_{24}(z) = \gamma$. Starting from an initial guess of γ, the Fermi energy can be estimated by solving eq. (21) with the false position method. Using this tentative value of the Fermi energy, the charge density at 32 randomly chosen grid points has been calculated by a truncated 200-steps recursion chain, and the first chain terminator $t_{24}(z)$ has been fitted in order to reproduce the charge density at these sampling points. This new terminator leads to a better estimate of the Fermi energy, and the procedure is repeated until self-consistency is reached. Usually only a few iterations are needed in order to get a simultaneous evaluation of the Fermi energy and the terminator.

After a final calculation of the charge density, a new effective potential is obtained by adding the Coulomb potential and the exchange-correlation potential to the bare ionic pseudopotential. The Coulomb potential has been calculated by solving Poisson's equation in reciprocal space, using a nearest-neighbour discretization of the laplacian. The local density approximation for the exchange-

correlation potential, with the parametrization proposed by Perdew and Zunger [15], has been used. A linear mixing of the new effective potential and the old one yields the starting potential for a new iteration of the self-consistent scheme, and the whole procedure is repeated until input and output potentials agree to within 0.001 Ryd.

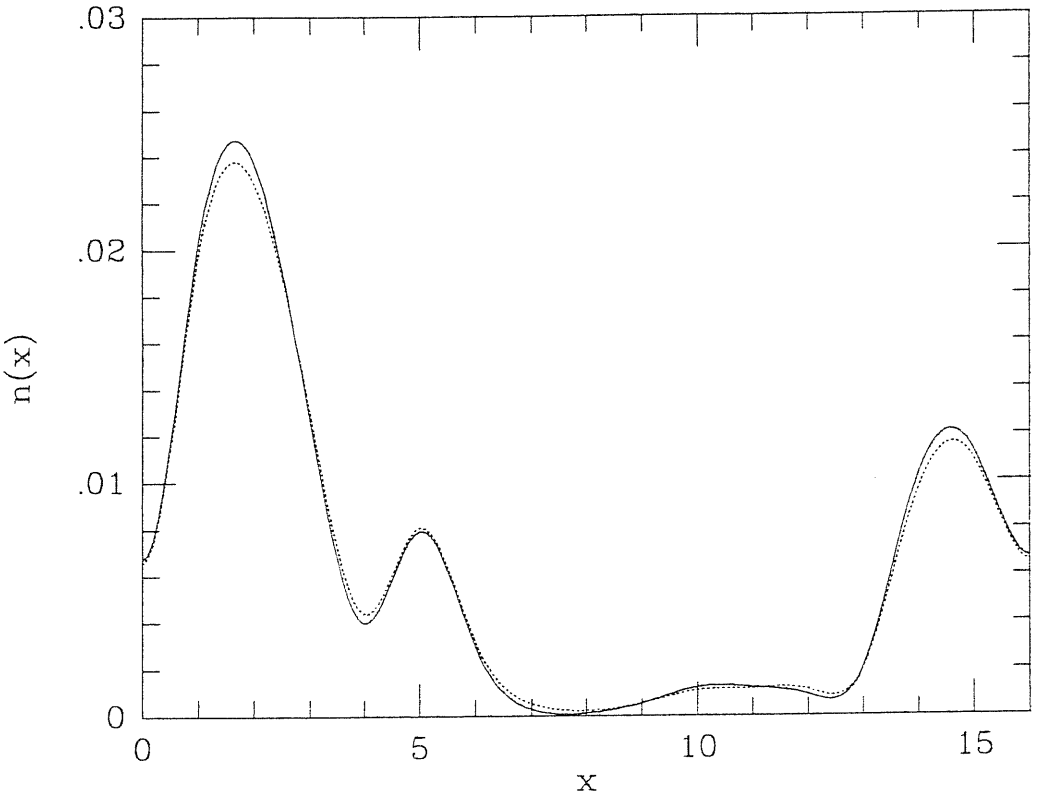

Fig. 6 – *Self-consistent charge density along the (111) direction obtained from a conventional orbital calculation (solid line) and from our approach (dotted line).*

The self-consistent charge density along the (111) direction is plotted in Fig. 6 (dotted line). For comparison, the self-consistent charge density obtained

from a conventional orbital calculation is also shown in Fig. 6 (solid line). The difference between the two results is almost entirely due to the approximate form of the terminator; actually, the mean square deviation is $\sigma = 3.6 \times 10^{-4}$, which compares favourably with the value of 4.9×10^{-4} obtained after the first iteration of the self-consistent scheme. Therefore, we conclude that our method is well suited for the self-consistent calculation of the charge density.

Conclusions and perspectives

In this work we have discussed a new method, based on the Green's function formalism, which leads directly to the charge density without invoking orbitals. From a computational point of view, the required workload scales linearly with the size of the system; moreover, no assumptions are made about the symmetry of the problem. Therefore, our method should turn out to be extremely efficient for the self-consistent calculation of ground-state properties of large, disordered systems.

Actually, our present algorithm, though not very demanding in terms of computer storage, is hardly convenient for systems with less then a few hundreds atoms per unit cell, if compared with the well-established plane waves approach. Anyway, we feel that a more reliable approach to grid coarsening, together with a general improvement of the algorithm, would lead to a speed up of two orders of magnitude or more.

In this respect, we are presently investigating a block renormalization approach to the calculation of the terminator. The idea is to partition the real-space grid into a number of small, non-overlapping blocks, and to diagonalize the hamiltonian separately for each block, in order to obtain a set of orthonormal, localized basis functions. Taking these states up to a given energy cutoff yields a new basis set which should allow a quick evaluation of the terminator while retaining the low-energy features of the spectrum.

Furthermore, a quite straightforward extension of the algorithm to non uniform real-space grids should make feasible, with little extra computational cost, all-electron calculations of ground state properties.

References

[1] W. Yang, Phys. Rev. Lett. **59**, 1569 (1987)

[2] W. Yang, Phys. Rev. A **38**, 5494 (1988)

[3] P. Cortona, Phys. Rev. B **44**, 8454 (1991)

[4] W. Yang, Phys. Rev. Lett. **66**, 1438 (1991)

[5] W. Yang, J. Chem. Phys. **94** (2), 1208 (1991)

[6] W. Yang, Phys. Rev. A **44**, 7823 (1991)

[7] S. Baroni, P. Giannozzi, Europhys. Lett. **17** (6), 547 (1992)

[8] J. Friedel, Adv. Phys. **3**, 446 (1954)

[9] A.R. Williams, P.J. Feibelman, N.D. Lang, Phys. Rev. B **26**, 5433 (1982)

[10] R. Zeller, J. Deutz, P.H. Dederichs, Sol. State Comm. **44**, 993 (1982)

[11] R. Haydock, V. Heine, M.J. Kelly, J. Phys. C **5**, 2845 (1972)

[12] R. Haydock, V. Heine, M.J. Kelly, J. Phys. C **8**, 2591 (1975)

[13] D.W. Bullett, R. Haydock, V. Heine, M.J. Kelly, Solid State Phys. **35** (1980)

[14] J.A. Appelbaum, D.R. Hamann, Phys. Rev. B **8**, 1777 (1973)

[15] J. Perdew, A. Zunger, Phys. Rev. B **23**, 5048 (1981)